# Flux folded neutrino-nucleus cross sections at geo-neutrino and reactor neutrino energies


Vaitsa Tsakstara

*Technological institute of Western Makedonia*

*University of Ioannina*

**Greece**


*INTERNATIONAL SCHOOL OF NUCLEAR PHYSICS*
*Nuclei in the Laboratory and in the Cosmos*

*Erice-Sicily: September 16-24, 2014*

# Outline

1. Introduction
   - Low and Intermediate neutrino energy sources
   - Coherent and Incoherent $\nu$-nucleus processes (NC-CC)
2. Results
   - Incoherent cross sections
     - Original
     - Fluxes
     - Flux averaged cross sections
   - Coherent cross sections
     - Original
     - Folded
     - Fluxes
3. Summary-Conclusion and Outlook

# Low and Intermediate neutrino energy sources

- Laboratory neutrino sources
  (i) $\pi^{\pm}$-stopped neutrinos ($\varepsilon_\nu \lesssim$ 60 MeV)
  (ii) Reactor neutrinos ($\varepsilon_\nu \lesssim$ 10 MeV)
  (iii) SNS neutrinos (Spallation-Neutron-Sources) ($\varepsilon_\nu \lesssim$ 60 MeV)

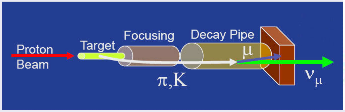


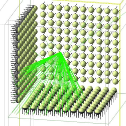

- Astrophysical neutrinos
  (i) Solar neutrinos ($\varepsilon_\nu \lesssim$ 18 MeV)
  (ii) Supernova neutrinos ($\varepsilon_\nu \lesssim$ 60-80 MeV)
  (iii) Geoneutrinos ($\varepsilon_\nu \lesssim$ 8 MeV)

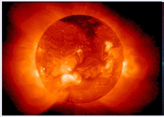

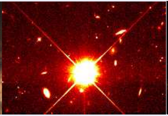

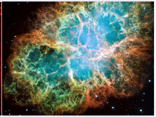

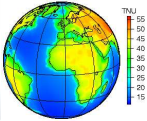

# Low and Intermediate neutrino energy spectra

The neutrino sources, astrophysical (solar, supernova, geo-neutrinos) and laboratory ($\beta$-beam, pion-muon stopped neutrino beams,beta-beam neutrinos reactor), with few exceptions, produce neutrinos that present a spectral distribution, characteristic of the source itself, and defined by

$$\frac{dN_\nu(\varepsilon_\nu)}{d\varepsilon_\nu} \equiv \eta(\varepsilon_\nu)$$

$N_\nu$ denotes the number of neutrinos of the beam.

Monochromatic beam neutrinos:

- the $\nu_\mu$ neutrino beam emerging from the $\pi^+$ decay at rest ($\varepsilon_\nu$= 29.8 MeV)
- the $^7Be$ solar neutrinos ($\varepsilon_\nu$= 0.862 MeV),

# Pion-muon decay at rest neutrinos

$\nu_e$, $\tilde{\nu}_e$ and $\nu_\mu$, $\tilde{\nu}_\mu$ are produced from the decay of $\pi^\pm$ and $\mu^\pm$ according to the reactions (slow pion and muon decay):

$$\pi^\pm \to \mu^\pm + \nu_\mu(\widetilde{\nu_\mu}) \qquad \mu^+ \to e^+ + \nu_e + \widetilde{\nu}_\mu$$

$$\pi^\pm \to e^\pm + \nu_e(\widetilde{\nu_e}) \qquad \mu^- \to e^- + \widetilde{\nu}_e + \nu_\mu$$

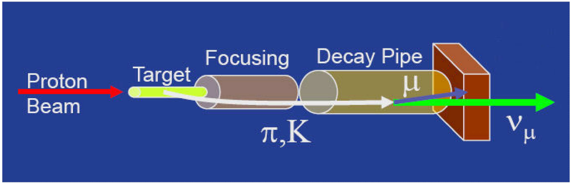


- The neutrinos of this source have energies $\varepsilon_\nu \precsim 52.8\text{MeV}$.
- Muon-factories (Fermilab, PSI, ...)

# Pion-muon decay at rest neutrino energy distributions

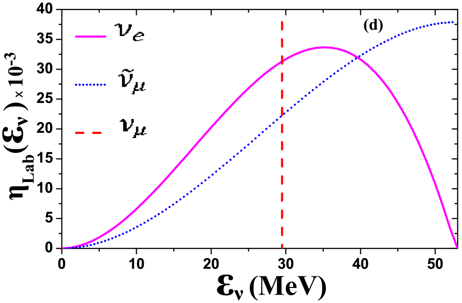


$$f_{\nu_e}(\varepsilon_{\nu_e}) = 96\varepsilon^2_{\nu_e}\, m_\mu^{-4}\, (m_\mu - 2\varepsilon_{\nu_e})$$

$$f_{\tilde{\nu}_\mu}(\varepsilon_{\tilde{\nu}_\mu}) = 16\varepsilon^2_{\tilde{\nu}_\mu}\, m_\mu^{-4}\, (3m_\mu - 4\varepsilon_{\tilde{\nu}_\mu})$$

- The $f_{\nu_e}$, $f_{\tilde{\nu}_\mu}$ useful in the parametrization of $SN$-$\nu$ (closed in high $\varepsilon_\nu$)
- $f_{\nu_\mu}$ → monochromatic, $\varepsilon_\nu \approx 29.2$ MeV

# Reactor neutrinos

B.R. Davis, P. Vogel, F.M. Mann, and R.E. Schenter, Phys. Rev. **C 19**, 2259 (1979).
Y. Declais *et al.*, Phys. Lett. **B 338**, 383 (1994)

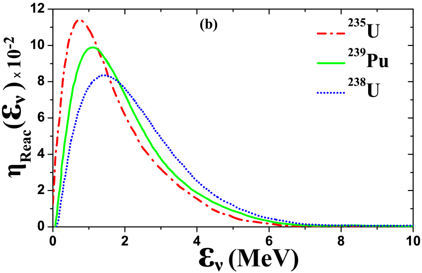


- In the fission of ${}^{235}U$, ${}^{239}Pu$, and ${}^{238}U$, neutron rich nuclei are produced and $\widetilde{\nu}_e$ anti-neutrinos are subsequently emitted via $\beta$ decay.

- Nuclear reactors, are sources of $\widetilde{\nu}_e$ which have an energy spectrum peaked at very low energies (the maximum peak is at about 0.5 MeV) and extending up to $\sim$ 10 MeV, characteristic of the $\beta^-$ decay of the fission products.

# Geoneutrinos

Geo-neutrinos are mainly $\widetilde{\nu}_e$ generated from $\beta$-decay nuclei. The reactions (decays) are accompanied by emission of an electron ($e^-$) and release of decay-energy ($Q_\beta$)

$$(A, Z) \to (A, Z+1) + e^- + \widetilde{\nu}_e + Q_\beta$$

- Most abundant radioactive groups isotopes of the present Earth are classified into three : (i) the $^{238}U$ decay series, (ii) $^{232}Th$ decay series, and (iii) $^{40}K$ isotope.
- The most recent measurements from KamLAND and Borexino are reaching the precision where they can start to constrain Earth models.

A. Gando *et al.* (KamLAND Collaboration), Nature Geo. **4**, 647 (2011).
G. Bellini *et al.* (Borexino Collaboration), Phys. Lett. **B 722**, 295 (2013)

# Geoneutrino energy spectra

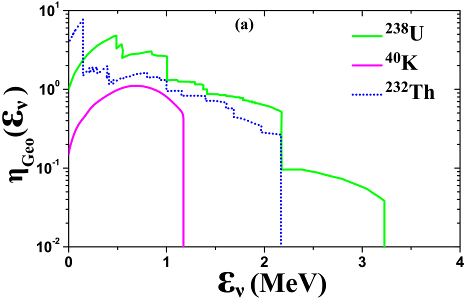


- $\widetilde{\nu}_e$ energy distributions coming from 82 beta decays in the U series,
- neutrino energy spectra coming from 70 beta decays Th series
- $^{40}K$ Geo-Neutrinos. Neutrinos from $^{40}K$ electron are also shown.
- Antineutrinos are generated by $\beta$-decays of all intermediate radioactive isotopes.

# Solar neutrinos

The solar neutrinos are $\nu_e$ neutrinos produced through weak, electromagnetic, and strong nuclear processes in the interior of our Sun.

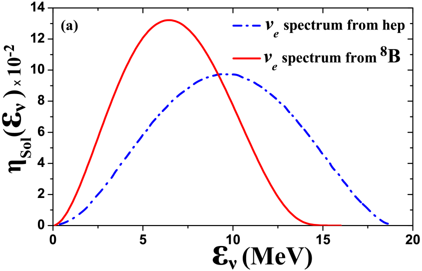


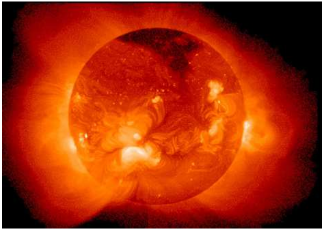

Measurements of the solar neutrino spectrum played a decisive role to clarify the solar neutrino puzzle and understand the neutrino oscillations.

# Supernova neutrinos

Nuclear processes, mediated by the weak-interaction, play an essential role during the collapse. While positron captures on nuclei and nuclear $\beta^+$ decays are also considered in supernova simulations, the two important weak processes are:

**Nuclear beta-decay**

$$(Z, A) \longrightarrow (Z+1, A) + e^- + \widetilde{\nu}_e$$

**electron capture**

$$(Z, A) + e^- \longrightarrow (Z-1, A) + \nu_e$$

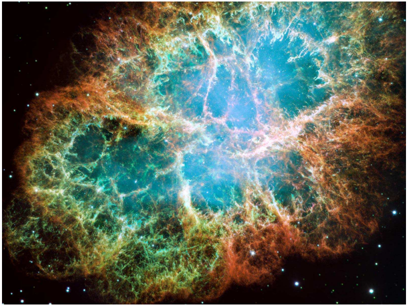

- Neutral current reactions (participate in the final SN-$\nu$ spectrum)

$$\nu(\tilde{\nu}) + e^{\pm} \longrightarrow \nu(\widetilde{\nu}) + e^{\pm} \qquad \nu(\tilde{\nu}) + (A, Z) \longrightarrow \nu(\widetilde{\nu}) + (A, Z)$$

# Supernova neutrino energy spectra

Neutrino energy-spectra emitted in core collapse SN are approximated as:

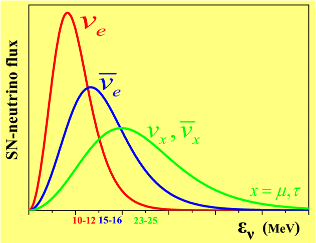


- $\langle \varepsilon_{\nu_e} \rangle < \langle \varepsilon_{\tilde{\nu}_e} \rangle < \langle \varepsilon_{\nu_x} \rangle$
- $R_{\nu_e} > R_{\tilde{\nu}_e} > R_{\nu_x}$

Average energy of emitted neutrinos reflects the temperature of matter around the neutrinosphere from where they escape

- $\nu_e$, $\widetilde{\nu}_e$ interact with matter via both CC and NC.
- $\nu_x$, $\widetilde{\nu}_x$ interact with matter only via NC.

In SN simulations various parametric expressions are used for SN-energy spectra.

# Supernova neutrino energy spectra

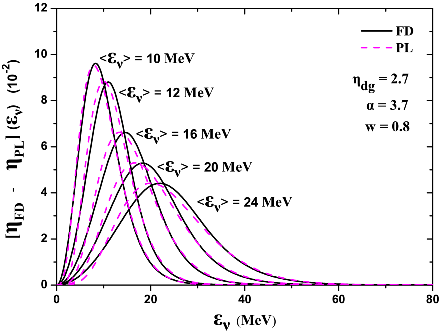


Both FD and PL yield similar distribution shapes characterized by the $T$ and the $\langle \varepsilon_\nu \rangle$

- $T$ = neutrino temperature
  $n_{dg}$ = degeneracy parameter
- $\langle \varepsilon_\nu \rangle$= mean neutrino energy,
  $\alpha$= piching parameter
- The width $w$ influence the high energy tail of the neutrino spectra

$$w = \frac{\sqrt{\langle \varepsilon_\nu^2 \rangle - \langle \varepsilon_\nu \rangle^2}}{w_0}$$

$$\eta_{FD}(\varepsilon_\nu) = N_2(n_{dg}) \frac{1}{T^3} \frac{\varepsilon_\nu^2}{1 + e^{(\varepsilon_\nu / T - n_{dg})}}$$

$$\eta_{PL}(\varepsilon_\nu) = C \left( \frac{\varepsilon_\nu}{\langle \varepsilon_\nu \rangle} \right)^\alpha exp \left( - \frac{(\alpha + 1)\varepsilon_\nu}{\langle \varepsilon_\nu \rangle} \right)$$

# Neutrino-Nucleus Cross section

There are 4 categories of neutrino-nucleus processes:

- charged-current neutrino-nucleus reactions

$$\nu_\ell + (A,Z) \longrightarrow (A,Z+1)^* + \ell^-$$
$$\widetilde{\nu}_\ell + (A,Z) \longrightarrow (A,Z-1)^* + \ell^+$$

- neutral-current neutrino-nucleus reactions

$$\nu + (A,Z) \longrightarrow (A,Z)^* + \nu'$$
$$\widetilde{\nu} + (A,Z) \longrightarrow (A,Z)^* + \widetilde{\nu}'$$

In the first two reactions, the signal is the outgoing lepton. In the latter two one possibility is the coherent (channel) detected by measuring the nuclear recoil, while the incoherent processes may be detected through the de-excitation products (signal is $\gamma$-ray, p or n release).

# Incoherent Neutrino-Nucleus Cross sections

Original Neutrino-Nucleus Cross sections are obtained from

$$\frac{\mathrm{d}^2\sigma}{\mathrm{d}\Omega[\mathrm{d}\omega]}\Big|_{\nu/\tilde{\nu}} = \frac{2G^2\varepsilon_f^2}{\pi(2J_i+1)}\cos^2\frac{\theta}{2}\delta(E_f - E_i - \omega)$$
$$\times \sum_{J=0}^{\infty} |\langle J_f \| \widehat{\mathcal{M}}_J(q) + \frac{\omega}{q}\widehat{\mathcal{L}}_J(q) \| J_i\rangle|^2$$
$$+ \quad \left[-\frac{1}{2}\frac{q_\mu^2}{q^2} + \tan^2\frac{\theta}{2}\right] \times \sum_{J=1}^{\infty}\left[\langle J_f \| \widehat{\mathcal{T}}_J^{mag}(q) || J_i\rangle|^2 + \langle J_f | \widehat{\mathcal{T}}_J^{el}(q) | J_i\rangle|^2\right]$$
$$\pm \quad 2\tan\frac{\theta}{2}\left[-\frac{q_\mu^2}{q^2} + \tan\frac{\theta}{2}\right]^{1/2} \sum_{J=1}^{\infty} \Re e \langle J_f || \widehat{\mathcal{T}}_J^{mag}(q) || J_i\rangle\langle J_f || \widehat{\mathcal{T}}_J^{el}(q) || J_i\rangle^*$$

$\theta$=scattering angle, $q$=3-momentumt ransfer, $q_\mu^2$=4-momentumt ransfer

# Coherent Neutrino-Nucleus Cross sections

For neutral current $\nu$-nucleus reactions the coherent ($gs \longrightarrow gs$) channel is possible. The angle differential cross section, $d\sigma/d\Omega$, of $\nu$-nucleus elastic-scattering on a nucleus (A,Z) is

$$\frac{d\sigma}{d\Omega} = \frac{G_F^2}{4\pi^2}\varepsilon_\nu^2(1 + cos\vartheta)\frac{Q_w^2}{4}\mathcal{F}(q^2)^2$$

$G_F$= the Fermi coupling constant
and $\mathcal{F}(q^2)$ contains the nuclear physics parameters:

$$\mathcal{F}(q^2) = \frac{1}{Q_w}\left[NF_N(q^2) - (1 - 4sin^2\Theta_w)ZF_Z(q^2)\right].$$

$F_Z(q^2)$ and $F_N(q^2)$, nuclear form factors for protons and neutrons.

# Coherent Neutrino-Nucleus Cross sections

$Q_w$ denotes the weak charge of the target nucleus

$$Q_w = N - (1 - 4sin^2\Theta_w)Z$$

$(sin^2\Theta_w \approx 0.231)$.
The g.s. (elastic) nuclear form factors $F_Z(q^2)$, for protons, and $F_N(q^2)$, for neutrons, are defined by

$$F_k(q^2) = \frac{k}{4\pi}\int j_0(qr)\rho_{n,p}(r)d^3r\,,\ \ k = N, Z$$

They are normalized as $F_{N,Z}(q^2 = 0) = 1$. The coherent cross section depends on quantity $\mathcal{F}(q^2)$, where the momentum transfer $q^2$ is given by

$$q^2 = 2\varepsilon_\nu^2(1 - cos\vartheta)$$

# Coherent Neutrino-Nucleus Cross sections

In early calculation the momentum dependence of the nuclear form factors was ignored by taking

$$F_N(q^2) \approx F_Z(q^2) \approx 1$$

Under such assuptions, and in this case the total coherent cross section, $\sigma_{tot}(\varepsilon_\nu)$, is approximately written as

$$\sigma_{tot}(\varepsilon_\nu) = \frac{G_F^2}{8\pi}\left[Z(4sin^2\Theta_W - 1) + N\right]^2 \varepsilon_\nu^2$$

Because

$$1 - 4sin^2\Theta_W \approx 0.04$$

(very small) earlier astrophysical calculations considered

$$\sigma_{tot} \propto N^2 \varepsilon_\nu^2$$

(ignoring the nuclear dependence)

# Original incoherent cross sections for $\nu$ and $\widetilde{\nu}$- *Te*, *Zn*, *Cd* scattering

$$\nu_\ell(\widetilde{\nu}_\ell) + (A, Z) \rightarrow (A, Z)* + \nu_\ell{}'(\widetilde{\nu}'_\ell)$$

The main Cd, Te, Zn isotopes at the detectors *CdZnTe* and *CdTe*, of COBRA and $TeO_2$, of CUORE experiments

| Isotope | $Z, N$ | Abudance (%) | Decay | $J^\pi(gs)$ |
|---|---|---|---|---|
| $^{128}Te$ | 52, 76 | 31.70 | Stable | $0^+$ |
| $^{130}Te$ | 52, 78 | 33.80 | Stable | $0^+$ |
| $^{112}Cd$ | 48, 72 | 24.00 | Stable | $0^+$ |
| $^{114}$Cd | 48, 74 | 28.80 | Stable | $0^+$ |
| $^{116}Cd$ | 48, 76 | 7.50 | $2\beta^-$ | $0^+$ |
| $^{64}Zn$ | 30, 34 | 48.63 | Stable | $0^+$ |
| $^{66}Zn$ | 30, 36 | 27.90 | Stable | $0^+$ |
| $^{70}Zn$ | 30, 40 | 0.62 | $2\beta^-$ | $0^+$ |

K. Zuber, Phys. Lett. **B 519**, 1 (2001); **B 571**, 148 (2003).
F.T. Avignone and Y.V. Efremenko, Nucl.Phys.B.Proc.Suppl. **87**, 304 (2000).

# Original total Cross-sections of $\nu$ and $\tilde{\nu}$ results of $^{64,66}Zn$

V. Tsakstara, T.S. Kosmas, J. Wambach, Prog. Part. Nucl. Phys. **66**, 424 (2011).
V. Tsakstara and T.S. Kosmas, Phys. Rev. **C 86**, 044618 (2012).

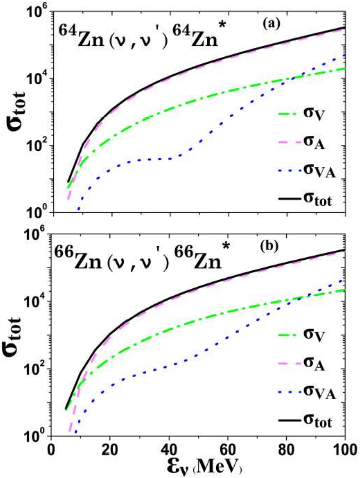


FIG. 2: Total cross sections, $\sigma_{tot}(\varepsilon_\nu)$, in units $10^{-42}\ cm^2$, for the reactions $^{64}Zn(\nu,\nu')^{64}Zn^*$ (up) and $^{66}Zn(\nu,\nu')^{66}Zn^*$ (down). The individual contributions of the polar-vector $\sigma_V$, the axial-vector $\sigma_A$ and their interference term $\sigma_{VA}$ are also illustrated.

- The corresponding curves of the two Zn isotopes, except a slight quantitative difference between the curves of the interference term $\sigma_{VA}(\varepsilon_\nu)$ in the region around $\varepsilon_\nu \approx 40$ MeV, show qualitative and quantitative similarity.
- For $\varepsilon_\nu \preceq$ 5-8 MeV, for both isotopes the polar-vector contribution $\sigma_V(\varepsilon_\nu)$ dominates while for high energies the axial-vector cross section $\sigma_A(\varepsilon_\nu)$ is approximately equal to the total cross section $\sigma_{tot}(\varepsilon_\nu)$.
- The polar vector contribution $\sigma_V$ is larger compared to that of the interference term, $\sigma_{VA}$, only for energies up to $\varepsilon_\nu \approx 80$ MeV.

# Original results $\nu$ and $\widetilde{\nu}$ - $^{128,130}Te$

V. Tsakstara and T.S. Kosmas, Phys. Rev. **C 83**, 054612 (2011)

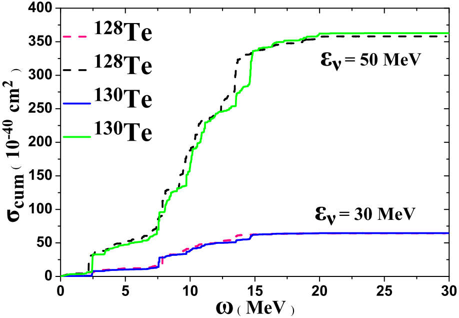


*Cumulative cross sections $\sigma_{cum}(\omega)$ for $^{128}Te$ and $^{130}Te$ for incoming neutrino*

- The $\sigma_{cum}(\omega)$ of $^{128}Te$ isotope, for $\omega \preccurlyeq$ 15 MeV, is a bit larger than that of $^{130}Te$, but for $\omega \succcurlyeq$ 15 MeV it occurs the opposite due to the fact that the dominant transitions of $^{128}Te$ lie at lower energies compared to those of $^{130}Te$
- The most abrupt increase (in both isotopes) is observed at $\omega \approx$ 15 MeV (the giant resonance region) and this is more clear in the case of $\varepsilon_{\nu}=$ 50 MeV.

# Nuclear responses to spectra of specific $\nu$-sources

For a connection of our results with the $\nu$-experiments, we carry out the folding of the calculated cross sections with the distribution $\eta(\varepsilon_\nu)$ of a specific $\nu$-source.

This way we estimated nuclear responses (signals to detectors) to various $\nu$- spectra.

These responses for the $d\sigma/d\omega(\omega,\varepsilon_\nu)$ and $\sigma_{tot}(\varepsilon_\nu)$ cross sections, are evaluated by

$$\frac{d\sigma}{d\omega}\Big|_{sign}(\omega) = \int_{\omega}^{\infty} \frac{d\sigma}{d\omega}(\omega,\varepsilon_\nu)\eta(\varepsilon_\nu)d\varepsilon_\nu$$

$$\sigma_{sign}(\varepsilon_\nu) = \sigma_{tot}(\varepsilon_\nu)\eta(\varepsilon_\nu)$$

Flux averaged cross sections $\langle\sigma_{tot}\rangle$ are obtained by using $\sigma_{tot}(\varepsilon_\nu)$.

$$\langle\sigma_{tot}\rangle = \int \sigma_{tot}(\varepsilon_\nu)\eta(\varepsilon_\nu)d\varepsilon_\nu$$

ANALYZING ASTROPHYSICAL NEUTRINO SIGNALS USING

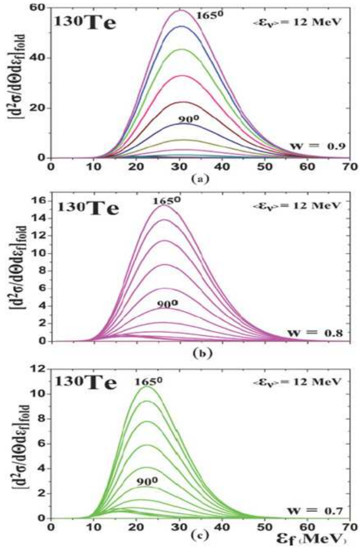


FIG. 3. (Color online) Convoluted double-differential cross sections $[d^2\sigma(\theta, \varepsilon_f)/d\Theta d\varepsilon_f]_{\rm fold}$ ($\times 10^{-40}$ cm$^2$ MeV$^{-1}$ rad$^{-1}$) versus the outgoing neutrino energy $\varepsilon_f$ for $\nu$ scattering on $^{130}$Te obtained by using the two-parameter FD distribution with fixed mean neutrino

- ***The high energy tail plays a significant role in the response of the detector.***
- ***Decreasing the width:***
  - ***reduces the cross section***
  - ***the energy maximum of the distribution is shifted to higher values***
- ***For w=0.9 in the range about the peak the folded cross section becomes a factor of about 4 larger compared to that for w=0.8.***

***V.T., T.S. Kosmas, PRC 84(2011) 064620***

***V.T., T.S.Kosmas, PRC 83(2011)054612***

V.Tsakstara., T.S. Kosmas, PRC 84(2011) 064620

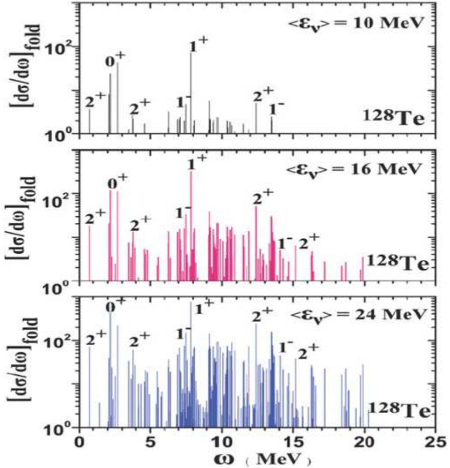


FIG. 4. (Color online) Convoluted single-differential cross section $[d\sigma(\omega)/d\omega]_{\rm fold}$ versus the excitation energy $\omega$ ($\times 10^{-40}$ cm$^2$ MeV$^{-1}$), averaged over a two-parameter FD spectral distribution ($w = 0.8$, $n_{\rm dg} = 2.7$, or $\alpha = 3.7$) with $\langle\varepsilon_\nu\rangle = 10$ MeV, $T = 2.58$ MeV (upper panel); $\langle\varepsilon_\nu\rangle = 16$ MeV, $T = 4.14$ MeV (middle panel); or $\langle\varepsilon_\nu\rangle = 24$ MeV, $T = 6.20$ MeV (lower panel).

- ***In all cases there is a rich nuclear response in the range of the discrete spectrum ($\omega$ < 7-8 MeV), but also in the continuum spectrum.***
- ***By increasing the mean energy $<\varepsilon_\nu>$ and keeping the width $w$ fixed the folded cross-section increases drastically throughout the excitation spectrum.***
- ***The excitation spectrum of SN-ν is fragmented over the states.***
- ***Inelastic ν- scattering excites the spin response, which is responsible for the $1^{-1}$ transitions around 8 and 14 MeV.***

# Neutrino Fluxes for $^{128,130}Te$ isotopes

Using $\sigma(\varepsilon_\nu)$ we estimated $\nu$-fluxes, $\Phi_\nu$, or scattering event rates, $N_{event}$, for the CUORE and COBRA detectors.
If $N_{Te}$ is the total number of nuclei (atoms) of $^{128}Te + ^{130}Te$ in the detector we have

$$\frac{dN_\nu}{dt} \equiv N_{event} = N_{Te}\Phi_\nu(\varepsilon_\nu)\sigma_{tot}(\varepsilon_\nu)$$

The CUORE detector is expected to have 988 crystal bolometers of $TeO_2$ or a total mass of $^{128}$Te+$^{130}$Te isotopes about $m_{Te} = 392$ kg translates to a number of atoms

$$N_{Te} = N_{^{128}Te} + N_{^{130}Te} = 1.85 \times 10^{27}$$

For $\varepsilon_\nu = 50$ MeV, the N-C scattering cross section is $\sigma^{max}_{cum}(50MeV) = 3.62 \times 10^{-38} cm^2$.
For a detection rate of $N_{event} = 1\ event\ hr^{-1}$, the resulting $\nu$ flux is

$$\Phi_\nu(\varepsilon_\nu = 50MeV) \approx 4.1 \times 10^6\ cm^{-2}s^{-1}$$

# Neutrino fluxes for $^{128,130}Te$ isotopes

Similarly, for $\varepsilon_\nu = 30$ MeV we have $\sigma_{cum}^{max}(30\,MeV) = 0.65 \times 10^{-38} cm^2$ and the corresponding neutrino flux is

$$\Phi_\nu(\varepsilon_\nu = 30 MeV) \approx 2.3 \times 10^7\, cm^{-2}\, s^{-1}$$

# Flux averaged cross sections for $^{66}Zn$

V. Tsakstara and T.S. Kosmas, Phys. Rev. **C 86**, 044618 (2012)

| | Fermi-Dirac (FD) | | | | | |
|---|---|---|---|---|---|---|
| $w$ | $\eta_{dg}$ | $T$ (MeV) | $\langle \sigma_V \rangle$ | $\langle \sigma_A \rangle$ | $\langle \sigma_{VA} \rangle$ | $\langle \sigma_{tot} \rangle$ |
| | | 2.13870 | 0.455 | 1.012 | 0.054 | 1.530 |
| | | 2.56644 | 0.730 | 2.241 | 0.094 | 3.056 |
| 0.7 | 4.4014 | 3.42193 | 1.573 | 7.162 | 0.203 | 8.863 |
| | | 4.27741 | 2.925 | 16.619 | 0.354 | 19.712 |
| | | 5.13289 | 4.931 | 32.197 | 0.585 | 37.361 |
| | | 2.58504 | 0.500 | 1.314 | 0.060 | 1.873 |
| | | 3.10205 | 0.801 | 2.819 | 0.102 | 3.704 |
| 0.8 | 2.7054 | 4.13607 | 1.750 | 8.700 | 0.217 | 10.573 |
| | | 5.17009 | 3.272 | 19.868 | 0.399 | 23.322 |
| | | 6.20410 | 5.526 | 38.203 | 0.753 | 44.032 |
| | | 2.98005 | 0.545 | 1.675 | 0.066 | 2.282 |
| | | 3.57606 | 0.885 | 3.506 | 0.110 | 4.475 |
| 0.9 | 1.1339 | 4.76808 | 1.950 | 10.530 | 0.238 | 12.611 |
| | | 5.96011 | 3.675 | 23.755 | 0.480 | 27.641 |
| | | 7.15213 | 6.197 | 45.280 | 1.027 | 51.890 |

Flux averaged cross sections (in units $10^{-42}$ $cm^2$) for the $^{66}Zn$ isotope obtained by using various SN-neutrino scenarios described by the two-parameter FD spectral distribution. The influence of the temperature T on the folded cross sections in the parameterizations used is evident.

# Coherent $\nu$-nucleus scattering

The N-C scattering of low and intermediate energy $\nu_l$ and $\widetilde{\nu}_l$, $l = l, \mu, \tau$,on the most abundant Cd isotopes of the COBRA experiment, i.e. $^{112}$Cd (abundance 24 %), $^{114}$Cd (abundance 28.8 %) and the $^{116}$Cd (abundance 7.5 %) isotopes, are represented by the reactions

$$\nu_l(\widetilde{\nu}_l) + {}^{112,114,116}Cd \rightarrow {}^{112,114,116}Cd + \nu_l'(\widetilde{\nu}_l')$$

# Coherent $\nu$-nucleus scattering for $^{112,114,116}Cd$

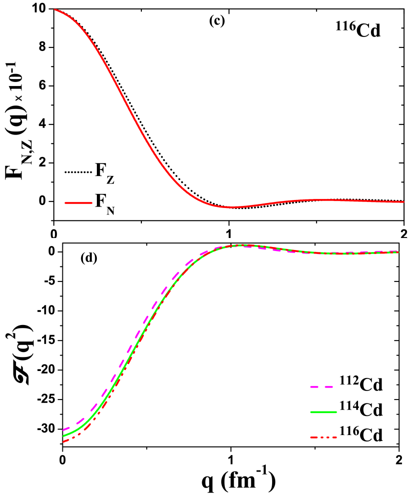


q dependence of:

- ground-state elastic nuclear form factors $F_{N,Z}(q^2)$
- form factor $\mathcal{F}(q^2)$ for $Cd$ isotopes

$$\mathcal{F}(q^2) = \frac{1}{Q_w}\Big[NF_N(q^2) - (1 - 4sin^2\Theta_w)ZF_Z(q^2)\Big].$$

# Original coherent cross sections for $^{112,114,116}Cd$

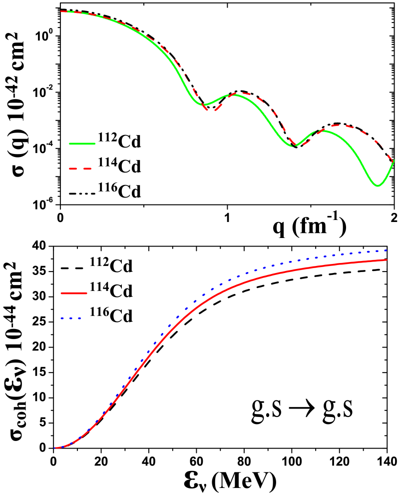


- Coherent total cross section for the N-C reactions $^{112,114,116}\mathrm{Cd}(\nu_l, \nu_l')^{112,114,116}\mathrm{Cd}^*$ as a function of momentum transfer $q$ and $\varepsilon_\nu$.
- The original cross sections are used below for evaluations of flux averaged folded cross sections for various neutrino sources.
- In general the differences are rather small.

# Flux averaged coherent cross sections for $^{112,114,116}Cd$

| Flux Averaged Cross Sections $\langle \sigma_{coh} \rangle$ ($10^{-42}$ $cm^2$) | | | | | | | | |
|---|---|---|---|---|---|---|---|---|
| Isotope | Geo-Neutrinos | | | Reactor Neutrinos | | | Solar Neutrinos | |
| | $^{40}$K | $^{238}$U | $^{232}$Th | $^{235}$U | $^{238}$U | $^{239}$Pu | $^{8}$B | hep |
| $^{112}Cd$ | 141.83 | 1409.52 | 911.22 | 180.11 | 476.82 | 9000.57 | 7969.87 | 9333.28 |
| $^{114}Cd$ | 151.38 | 1504.40 | 972.56 | 192.20 | 508.90 | 9604.36 | 8503.99 | 9956.57 |
| $^{116}Cd$ | 161.24 | 1602.38 | 1035.91 | 204.71 | 542.02 | 10227.68 | 9055.25 | 10597.82 |

Flux averaged coherent cross sections $\langle \sigma_{coh} \rangle$ (in units $10^{-40}$ $cm^2$) for $^{112}$Cd, $^{114}$Cd and isotopes $^{116}$Cd obtained in the case of neutrino energy-spectra coming from two neutrino sources: (i)Geo-neutrinos, (ii) Reactor neutrinos and (iii) Solar neutrinos.

# Fluxes for $^{114}Cd$ isotope

By using our theoretical cross sections $\sigma(\varepsilon_\nu)$, we estimate the signals created on $Cd$ detector given by the expression

$$\sigma_{sign}(\varepsilon_\nu) = \sigma_{coh}(\varepsilon_\nu)\eta(\varepsilon_\nu)$$

We may also evaluate the $\nu$-fluxes $\Phi_\nu$ or the scattering event rates, $N_{event}$, for the COBRA detector.
For a mass 100 Kgr of detector material $CdZnTe$ or $CdTe$ and a typical detection rate of $N_{event} = 1$ event $hr^{-1}$, we have

$$\frac{dN_\nu}{dt} \equiv N_{event} = N_{Cd}\Phi_\nu(\varepsilon_\nu)\sigma_{tot}(\varepsilon_\nu)$$

$N_{Cd}$ is the total number of nuclei (atoms) of $^{114}Cd$ in the detector.

# Coherent fluxes of $\nu$-$^{114}Cd$

Coherent neutrino fluxes $\Phi_\nu(\varepsilon_\nu)$ for $^{114}$Cd isotope for the materials *CdTe* and *CdZnTe* (COBRA experiment) obtained for SN neutrinos with mean energies $\langle\varepsilon_\nu\rangle = 12$, 16 and 24 MeV. $N_0$ is the Avogadro's number.

| Coherent $\nu$-fluxes $\Phi_\nu$ (in $10^9\, sec^{-1}\ cm^2$) | | | | |
|---|---|---|---|---|
| Detector Medium | Number of Atoms | $^{114}Cd$ (Kgr) | $\langle\varepsilon_\nu\rangle$ (MeV) | $\Phi_\nu$ |
| *CdTe* | 120.11 $N_0$ | 13.5 | 12<br>16<br>24 | 1.447<br>0.862<br>0.449 |
| *CdZnTe* | 94.17 $N_0$ | 10.6 | 12<br>16<br>24 | 1.847<br>1.100<br>0.566 |

# Summary-Conclusion and Outlook

- Our Incoherent $\nu$-Te cross sections are encouraging for using Te as $\nu$-detector in experiments like CUORE, COBRA (main goal $0\nu\beta\beta$ decay search).
- The above $\nu$-fluxes are of the same order with those expected at the Spallation Neutron Source at ORLaND, Oak Ridge.
- Similar conclusions are extracted from the calculations of $^{64,66}Zn$, isotopes, content of the semi-conductor CdZnTe (COBRA exp.).
- Our present results for $^{40}$Ar show that for incoming $\nu$ energies higher than $\varepsilon_\nu \sim 30$ MeV, the incoherent channel is not negligible and explicit nuclear reaction calculations are necessary (Shell Model, QRPA, etc.)
- The main advantage of the neutral current $\nu$-nucleus processes lies in the presence of the coherent effect of all neutrons in the target.
- The detection of galactic SN-$\nu$ by employing rather small size spherical TPC detector filled with a high pressure noble gas ($Ar$, etc.) is promising (Coherent scattering).

# Thank you!!!


Isola di Sicilia
Palermo
Scopello di Castellammare
Cefalu
S. Stefano di Camastra
Messina
Taormina
Catania
Erice
Trapani
Polizzi Generosa
Resuttano
Caltagirone
Marsala
S. Elisabetta
Agrigento
Noto
Mare di Mediterraneo